The Canadian Mineralogist
Vol. 34, pp. 147-159 (1996)

INTRINSIC AND EXTERNAL CONTROLS ON THE INCORPORATION OF RARE-EARTH ELEMENTS IN CALC-SILICATE MINERALS

YUANMING PAN

Department of Geological Sciences, University of Saskatchewan, Saskatoon, Saskatchewan S7N 5E2

MICHAEL E. FLEET

Department of Earth Sciences, University of Western Ontario, London, Ontario N6A 5B7

ABSTRACT

The rare-earth elements (*REE*) in twenty nine calc-silicate minerals, mostly of metamorphic or hydrothermal origin, and catapleiite have been analyzed by inductively coupled plasma – mass spectrometry (ICP–MS). Using pure mineral separates, very low detection limits for *REE* in minerals (3 to 54 ppb) are achieved, and *REE* patterns for some minerals with low abundances of *REE* are reported for the first time. The chondrite-normalized *REE* patterns of the calc-silicate minerals vary significantly. Although external geochemical factors are important in determining the *REE* characteristics of metamorphic and hydrothermal calc-silicate minerals, crystal-chemical effects are resolved also. A consideration of stereochemical environments of the Ca site(s) allows the formulation of qualitative rules for selectivity of *REE* and site occupancy in calc-silicate minerals. The selectivity of *REE* is controlled largely by the size of the Ca position: in calc-silicate minerals with multiple Ca sites, bond-valence calculation is a powerful first-approximation technique for predicting the site preference of *REE*.

Keywords: rare-earth elements, ICP–MS, calc-silicate minerals, substitution, bond-valence calculations, crystal-chemical controls, external controls.

SOMMAIRE

La teneur en terres rares de vingt-neuf calc-silicates, surtout d'origine métamorphique ou hydrothermale, et de la catapléiite a été établie par analyse au plasma avec couplage inductif combiné à la spectrométrie de masse. En utilisant des concentrés de minéraux purifiés, il est possible d'atteindre des seuils de détection très faibles, de 3 à 54 ppb; les spectres de terres rares de certains de ces minéraux ayant de très faibles teneurs en terres rares sont présentés pour la première fois. Les spectres de terres rares des calc-silicates, normalisés par rapport aux teneurs chondritiques, démontrent un très grande variabilité. Quoique les facteurs géochimiques imposés par le milieu sont importants pour établir la teneur en terres rares des calc-silicates métamorphiques et hydrothermaux, nous parvenons aussi à définir des effets cristallochimiques. Une considération du milieu stéréochimique du (ou des) site(s) de Ca mène à la formulation de règles qualitatives pour établir la sélectivité des terres rares et l'occupation des sites des calc-silicates. Cette sélectivité dépend surtout de la taille de la position qu'occupe le Ca; dans les cas où le Ca peut occuper une multiplicité de sites, un calcul de la valence de liaison mène à une prédiction qualitative de la préférence des terres rares pour un site quelconque.

(Traduit par la Rédaction)

Mots-clés: terres rares, analyse par plasma à couplage inductif avec spectrométrie de masse, calc-silicates, substitution, valence de liaison, contrôle cristallochimique, contrôle externe.

INTRODUCTION

Knowledge of the distribution of rare-earth elements (*REE*) in minerals is important to understand the behavior of these elements in geological processes. Significant progress in documenting the distribution of the *REE* in minerals of igneous systems has been made during the past twenty years and has furnished much insight into magmatic petrogenesis (McKay 1989, and references therein). Although *REE* geochemistry has been applied extensively to studies of metamorphism and hydrothermal alteration (Grauch 1989, Lottermoser 1992, and references therein), very few data exist for *REE* in rock-forming minerals of metamorphic and hydrothermal systems (Grauch 1989), with the exception of some *REE*-rich minerals (*e.g.*, apatite, calcite, fluorite, and titanite; Möller & Morteani 1983, Ayers & Watson 1993, Pan *et al.* 1994, Fleet & Pan 1995a). The distribution of minor and trace amounts of *REE* in nature is dominated by their

substitution for Ca (*e.g.*, Fleet & Pan 1995a, b). Fleet & Pan (1995a) showed that bond-valence calculation is a powerful first-approximation technique for deducing the site preference of the *REE* in end-member calc-silicate minerals having structures with multiple Ca positions, and that the *REE* characteristics of fluorapatite and some metamorphic calc-silicate minerals are consistent with prediction from bond valence and average Ca–O,OH,F bond distance (*i.e.*, size of Ca position).

In this paper, we report on the abundances of *REE* in calc-silicate minerals, mostly of metamorphic or hydrothermal origin, and catapleiite, by inductively coupled plasma – mass spectrometry (ICP–MS) analysis. Most of these calc-silicate minerals are commonly major constituents of various metamorphic and hydrothermal assemblages but have not been examined previously for their trace element contents. Their observed *REE* patterns are analyzed using size of Ca position and bond valence for crystal-chemical control. In many cases, factors external to the mineral (bulk composition, fluid composition, T, P, *etc.*) are apparently more influential in determining the *REE* characteristics.

Mineral Specimens and Analytical Procedures

A total of 31 specimens, representing 29 calc-silicate mineral species and catapleiite (Table 1), were selected from mineral collections at the Department of Earth Sciences, University of Western Ontario, and the Department of Geological Sciences, University of Saskatchewan. These mineral species encompass a

TABLE 1. LIST OF MINERALS INVESTIGATED

Mineral formula	Number	Locality	Origin
Åkermanite, $Ca_2MgSi_2O_7$	UWO3461	Crestmore, California	metamorphic
Andradite, $Ca_3Fe_2(SiO_4)_3$	A5.6	San Benito, California	hydrothermal
Anorthite, $CaAl_2Si_2O_8$	F3.13	Miakejima, Japan	hydrothermal
Apophyllite, $KCa_4Si_8O_{20}(F,OH)\cdot 8H_2O$	no number	Broken Hill, N.S. Wales	metamorphic
Axinite, $(Ca,Mn,Fe)_3Al_2BSi_4O_{15}(OH)$	UWO1058	Mineral County, Nevada	hydrothermal
Bustamite, $(Ca_{0.78}Mn_{0.12}Fe_{0.1})_2Si_2O_6$	no number	Broken Hill, Australia	metamorphic
Catapleiite, $Na_2ZrSi_3O_9\cdot 2H_2O$	UWO2265	Barkevik, Norway	magmatic
Clinozoisite, $Ca_2Al_3(Si_2O_7)(SiO_4)O(OH)$	B15.1	Hollinger mine, Ontario	hydrothermal
Datolite, $CaBSiO_4(OH)$	UWO2188	West Paterson, New Jersey	hydrothermal
Diopside, $CaMgSi_2O_6$	A5.6	San Benito, California	hydrothermal
Epidote[1], $Ca_2FeAl_2(Si_2O_7)(SiO_4)O(OH)$	UWO3311	Munro Twp, Ontario	metamorphic
Epidote[2], $Ca_2FeAl_2(Si_2O_7)(SiO_4)O(OH)$	UWO3345	Wollaston Twp, Ontario	metamorphic
Gehlenite, $Ca_2Al(AlSi)O_7$	UWO3164	Oka, Quebec	magmatic
Grossular, $Ca_3Al_2(SiO_4)_3$	A5.4	Asbestos, Quebec	hydrothermal
Heulandite, $(Ca,Na_2)Al_2Si_7O_{18}\cdot 6H_2O$	UWO832	Paterson, New Jersey	hydrothermal
Ilvaite, $CaFe_2FeOSi_2O_7(OH)$	UWO3061	Lembi County, Idaho	hydrothermal
Larnite, β-Ca_2SiO_4	A4.1	Larne, North Ireland	metamorphic
Laumantite, $CaAl_2Si_4O_{12}\cdot 4H_2O$	UWO3814	West Bay, Nova Scotia	hydrothermal
Margarite, $CaAl_2(Al_2Si_2)O_{10}(OH)_2$	UWO78	unknown	
Merwinite, $Ca_3Mg(SiO_4)_2$	UWO3470	Crestmore, California	metamorphic
Monticellite, $CaMgSiO_4$	UWO3468	Crestmore, California	metamorphic
Pectolite, $NaCa_2Si_3O_8(OH)$	UWO1386	West Paterson, New Jersey	hydrothermal
Prehnite, $Ca_2Al_2Si_3O_{10}(OH)_2$	UWO264	Upper Montclair, New Jersey	hydrothermal
Scapolite, $(Na,Ca)_4(Al,Si)_{12}O_{24}(Cl,CO_3,SO_4)$	ON70	Bancroft, Ontario	metamorphic
Spurrite, $Ca_5(SiO_4)_2(CO_3)$	UWO3475	Crestmore, California	metamorphic
Stilbite, $NaCa_2Al_5Si_{13}O_{36}\cdot 14H_2O$	UWO2664	Linn County, Oregon	hydrothermal
Tilleyite, $Ca_5Si_2O_7(CO_3)_2$	UWO3478	Crestmore, California	metamorphic
Titanite, $CaTiSiO_5$	no number	Westport, Ontario	pegmatitic
Tremolite, $Ca_2(Mg,Fe)_5Si_8O_{22}(OH)_2$	UWO2203	Marbridge Mine, Quebec	hydrothermal
Vesuvianite, $Ca_{19}(Al,Mg)_{13}B_{0-5}Si_{18}O_{68}(OH,O,F)_{10}$	UWO2653	Mexico	metamorphic
Wollastonite, $CaSiO_3$	UWO3375	Balmat, New York	metamorphic

Minerals from the collection of the University of Western Ontario are designated UWO; other minerals are from the mineral collection of the University of Saskatchewan. Attempts to separate lawsonite and pumpellyite were unsuccessful.

TABLE 2. COMPARISON OF THREE INTERNATIONAL STANDARDS AND ESTIMATED DETECTION LIMIT

Standard	BHVO-1			BIR-1			SY-2			Det Lim
Elements	1	2	3(%)	1	2	3(%)	1	2	3(%)	
La (ppm)	15.9	15.8	0.6	0.62	0.6	3.3	72	75	-4.0	0.018
Ce	38.3	39	-1.8	1.92	1.87	2.7	169	175	-3.4	0.014
Pr	5.34	5.7	-6.3	0.36	0.36	0	19.3	18.8	2.7	0.004
Nd	25.0	25.2	-0.8	2.37	2.3	3.0	74	73	1.4	0.054
Sm	6.37	6.2	2.7	1.15	1.06	8.5	16.0	16.1	-0.6	0.024
Eu	2.21	2.06	7.3	0.53	0.56	-5.4	2.42	2.42	0	0.011
Gd	6.34	6.4	-0.9	1.9	1.73	9.8	16.9	17	-0.6	0.033
Tb	0.92	0.96	4.2	0.34	0.36	-5.6	2.69	2.5	7.6	0.004
Dy	5.53	5.2	6.3	2.56	2.69	-4.8	19.7	18	9.4	0.016
Ho	0.98	0.99	-1.0	0.55	0.61	-9.8	4.36	3.8	15	0.003
Er	2.51	2.4	4.6	1.64	1.7	-3.5	14.7	12.4	19	0.01
Tm	0.33	0.33	0	0.29	0.24	20.8	2.35	2.1	12	0.004
Yb	2.08	2.02	3.1	1.82	1.63	11.7	16.6	17	2.4	0.009
Lu	0.27	0.29	6.9	0.25	0.25	0	2.91	2.7	7.8	0.007

BHVO-1, BIR-1, SY-2 are three international standards. 1, analytical values; 2, recommended values of Govindaraju (1989); 3, difference (%, percent); "Det Lim" is detection limit.

wide spectrum of structure types, from orthosilicates to disilicates, ring silicates, chain silicates, phyllosilicates and framework silicates, and diverse mineral chemistry. Catapleiite, $Na_2Zr(Si_3O_9)\cdot 2H_2O$, is included in this study because a significant amount of Ca commonly substitutes for Na in this mineral. Although most of the specimens were already in the form of single crystals, all of them were subjected to an initial step of hand-picking at 60–70 mesh (0.0212–0.025 cm) size under a binocular microscope, followed by magnetic separation or heavy-liquid treatment (or both), and another step of hand-picking at 120–140 mesh (0.0105–0.0125 cm) size. Subsequently, all mineral separates were examined by a combination of optical microscopy, powder X-ray-diffraction analysis, back-scattered electron imaging, and quantitative electron-microprobe (EMP) analysis. These steps were taken to minimize impurities. Back-scattered electron imaging of polished grain mounts showed that impurities in all mineral separates are invariably much less than 1% and do not include any phases that typically are sinks for *REE* (*e.g.*, allanite, monazite, titanite and zircon; Pan *et al.* 1993, 1994).

The samples were analyzed for the major elements using a JEOL–8600 Superprobe equipped with three automated wavelength-dispersion spectrometers, at the University of Saskatchewan. Operating conditions included an accelerating voltage of 15 kV, a beam current of 10 nA, a counting time of 20 s, and mineral standards. Levels of concentration of 14 *REE* and 18 other trace elements were determined by inductively coupled plasma – mass spectrometry (ICP–MS; Perkin Elmer Sciex® Elan 5000) at the University of Saskatchewan, following the sample preparation procedure of Xie *et al.* (1994) and standard solution-ICP–MS analytical procedure of Jenner *et al.* (1990). All minerals considered in this study are digested readily in HF–HNO_3 within 48 hours, except for bustamite (72 hours). A comparison of analytical results and recommended concentrations of *REE* in three international standards is presented in Table 2. Detection limits for the *REE*, defined as 3σ of procedural blanks, are between 3 to 54 ppb (Table 2).

TABLE 3. RARE-EARTH-ELEMENT CONCENTRATIONS IN CALC-SILICATE MINERALS

	Ak	And	And†	An	Apo	Ax	Bst	Cat	Czo	Dat	Di
La (ppm)	11.7	0.21	0.2	0.62	0.5	0.74	0.53	209	0.28	31.7	0.63
Ce	11.3	2.41	2.26	1.52	0.42	0.83	1.31	413	0.76	20.4	1.54
Pr	1.78	0.66	0.59	0.21	0.05	0.07	0.2	37.5	0.12	1.26	0.19
Nd	7.08	2.52	2.2	0.71	0.06	0.13	0.97	98	0.52	3.92	0.75
Sm	1.59	0.2	0.21	0.11	0.02	0.03	0.41	17.1	0.23	0.41	0.06
Eu	0.42	0.63	0.56	0.09	0.01	0.03	0.94	1.58	0.75	0.4	0.04
Gd	2.11	0.16	0.1	0.14	0.03	0.12	0.73	19.6	0.51	0.35	0.1
Tb	0.31	0.01	0.01	0.01	0	0.03	0.13	6.16	0.12	0.02	0.01
Dy	2.44	0.1	0.11	0.05	0	0.35	0.96	73.4	1.17	0.14	0.06
Ho	0.57	0.01	0.02	0.01	0	0.12	0.2	22.0	0.33	0.02	0
Er	1.66	0.07	0.05	0.02	0	0.63	0.73	97.3	1.45	0.03	0
Tm	0.26	0.01	0.02	0	0	0.15	0.1	21.0	0.25	0	0
Yb	1.82	0.1	0.09	0	0	1.43	0.83	175	2.02	0	0
Lu	0.26	0.02	0.01	0	0	0.25	0.14	27.9	0.34	0	0
La_N/Yb_N	4.34	1.42	1.58			0.35	0.43	0.81	0.09		
Eu_N/Eu_N^*	0.70	10.8	11.8	2.22	1.25	1.53	5.25	0.26	6.69	3.23	1.58
Control	I	E	E	I	I	I	I	I	E	I	E

	Ep[1]	Ep[2]	Gh	Grs	Hsl	Ilv	Lrn	Lmt	Mrg	Mwn	Mtc
La (ppm)	0.63	16.65	294	0.06	0.35	3.24	19.9	0.13	0.18	2.67	0.38
Ce	1.39	58.7	443	0.2	0.04	1.82	22.5	0.3	0.15	5.94	0.47
Pr	0.21	11.61	42.3	0.02	0	0.65	5.34	0.02	0.02	0.91	0.09
Nd	1.14	62.1	140	0.13	0.03	3.2	25.6	0.07	0.07	4.32	0.48
Sm	0.56	11.25	16.5	0.63	0	0.78	6.15	0.03	0	1.4	0.11
Eu	7.01	10.99	4.4	0.2	0	0.24	1.7	0	0.02	0.29	0.03
Gd	1.57	7.99	11.9	2.51	0.14	1.23	7.69	0	0	1.72	0.19
Tb	0.36	1	0.99	0.64	0	0.18	1.02	0	0	0.3	0.04
Dy	3.78	5.93	4.51	4.87	0.03	1.44	6.31	0	0.02	2.07	0.46
Ho	1.13	1.15	0.7	1	0	0.33	1.26	0	0	0.44	0.11
Er	4.94	3.25	1.52	2.95	0.02	1.04	3.56	0	0	1.34	0.42
Tm	0.88	0.42	0.19	0.41	0	0.11	0.41	0	0	0.21	0.09
Yb	6.5	2.71	0.87	2.3	0.02	0.6	2.58	0	0	1.56	0.58
Lu	0.96	0.41	0.12	0.27	0	0.09	0.37	0	0	0.25	0.09
La_N/Yb_N	0.07	4.15	228	0.02	1.18	3.65	5.21			1.16	0.44
Eu_N/Eu_N^*	22.8	3.55	0.96	0.49		0.75	0.76			0.57	0.64
Control	E	I	I	I	I	I	I	I	I	I	I

	Pct	Prh	Scp	Spu	Stb	Tly	Tnt	Tr	Ves	Wo
La (ppm)	0.09	0.84	8.98	12.4	0.01	0.88	1685	1.2	957	2.32
Ce	0.38	0.86	20.05	20.9	1.72	1.06	4535	2.99	1142	6.85
Pr	0.06	0.15	2.72	3.98	0.05	0.09	749	0.39	75	0.92
Nd	0.48	0.73	12.52	17.5	0.03	0.24	3392	1.51	168	3.8
Sm	0.09	0.11	3.67	4.47	0.01	0.04	519	0.38	14.5	0.96
Eu	0.06	0.09	1.15	1.07	0.01	0.01	111	1.12	11.1	0.13
Gd	0	0.1	4.93	5.85	0.03	0.07	459	0.29	12.9	0.97
Tb	0	0.03	1.04	0.91	0	0.01	63	0.05	0.96	0.13
Dy	0	0.16	6.12	6.41	0	0.07	401	0.25	4.94	0.83
Ho	0	0.02	0.98	1.43	0	0.02	81	0.03	0.88	0.16
Er	0	0.05	2.23	4.28	0	0.1	260	0.07	2.53	0.48
Tm	0	0.01	0.28	0.57	0	0.02	40	0.01	0.36	0.07
Yb	0	0.06	1.56	3.57	0	0.19	277	0.1	2.34	0.59
Lu	0	0	0.17	0.52	0	0.04	40	0.01	0.33	0.08
La_N/Yb_N		9.46	3.89	2.35	0	3.13	4.11	8.11	276	2.66
Eu_N/Eu_N^*		2.63	0.83	0.64	0	0.58	0.69	10.3	2.48	0.41
Control	I	I	I	I	I	I	I	I	I	I

See Table 1 for number, locality and origin of minerals; Mineral abbreviations in addition to those of Kretz (1983): Cat, catapleiite; Dat, datolite; Ilv, ilvaite; Lrn, larnite; Spu, spurrite.†, duplicated analysis of andradite; ppm, parts per million; La_N/Yb_N, chondrite-normalized La/Yb ratio; $Eu_N^* = (Sm_N \times Gd_N)^{0.5}$; I, REE pattern consistent with intrinsic (crystal chemical) control; E, REE pattern indicative of external factors.

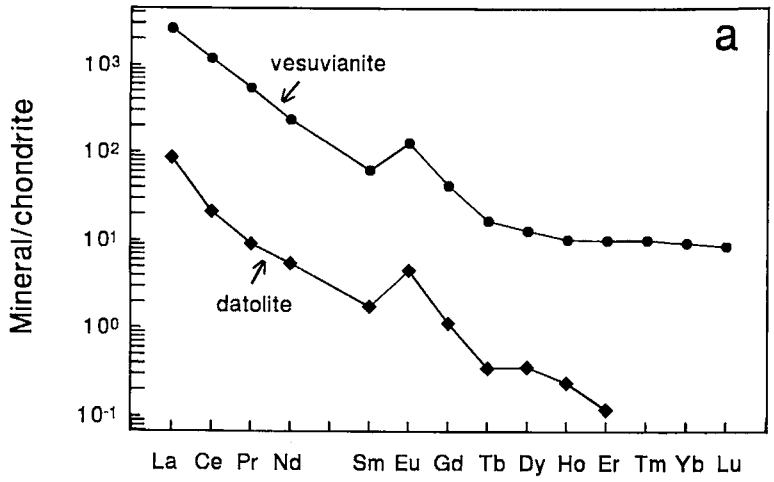
a
vesuvianite
datolite
Mineral/chondrite
10^3
10^2
10^1
10^0
10^{-1}
La Ce Pr Nd Sm Eu Gd Tb Dy Ho Er Tm Yb Lu

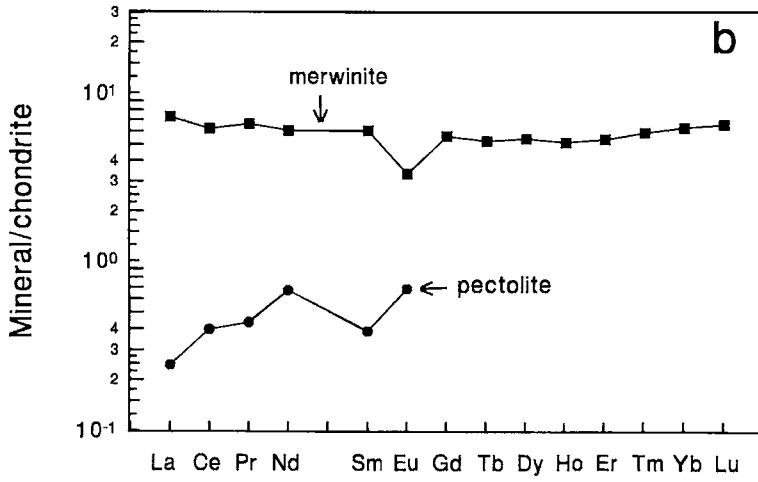
b
merwinite
pectolite
Mineral/chondrite
10^1
10^0
10^{-1}
La Ce Pr Nd Sm Eu Gd Tb Dy Ho Er Tm Yb Lu

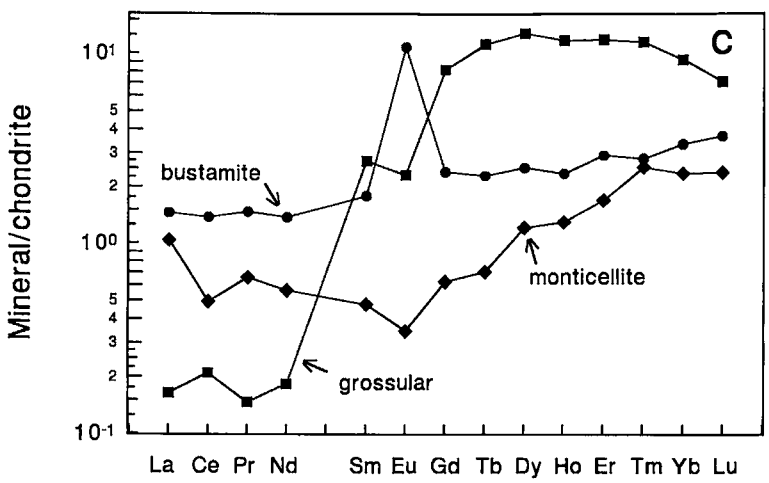
c
bustamite
monticellite
grossular
Mineral/chondrite
10^1
10^0
10^{-1}
La Ce Pr Nd Sm Eu Gd Tb Dy Ho Er Tm Yb Lu

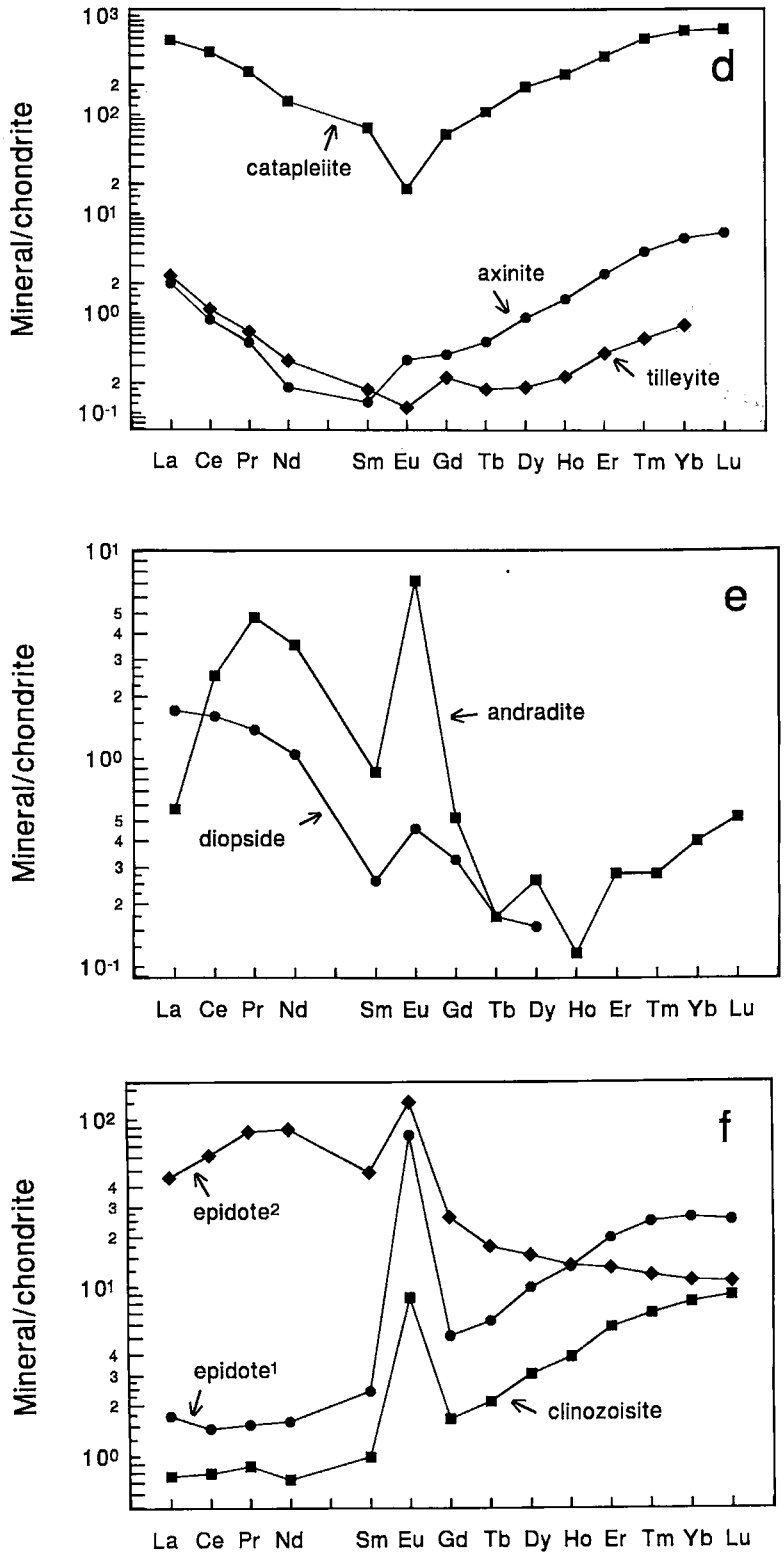

FIG. 1. Representative chondrite-normalized *REE* patterns of calc-silicate minerals: a) *LREE*-enriched (datolite and vesuvianite); b) flat (merwinite) and a partial one for pectolite; c) *HREE*-enriched (bustamite, grossular, and monticellite); d) convex-downward (axinite, catapleiite, and tilleyite); e) coexisting andradite and diopside from San Benito, California; and f) epidote-group minerals (see Table 1 for details). Chondrite values are those recommended by Taylor & McLennan (1985).

RESULTS

The concentrations of the *REE* in all minerals are given in Table 3. A complete list of EMP and ICP–MS analytical results for all mineral specimens (Table 4) is available from the Depository of Unpublished Data, CISTI, National Research Council of Canada, Ottawa, Ontario K1A 0S2.

The individual *REE* in calc-silicate minerals considered in this study exhibit a wide range in abundance (Table 3). The phyllosilicate minerals, including apophyllite and margarite, and zeolite-group minerals (heulandite, laumontite and stilbite) have the lowest *REE* abundances, typically less than 1 ppm of individual *REE* (Table 3). Four minerals (*i.e.*, catapleiite, gehlenite, titanite, and vesuvianite) are characterized by high levels of *REE*, with Ce in excess of 400 ppm in all four species.

The calc-silicate minerals exhibit a wide variation in chondrite-normalized *REE* patterns: 1) the light rare-earth elements (*LREE*) are enriched over the heavy rare-earth elements (*HREE*) (*e.g.*, datolite and vesuvianite; Fig. 1a); 2) the pattern is flat (*e.g.*, merwinite; Fig. 1b); 3) the *HREE* are enriched over the *LREE* (*e.g.*, bustamite, grossular, and monticellite; Fig. 1c), or 4) the pattern is convex-downward (*e.g.*, axinite, catapleiite, and tilleyite; Fig. 1d). The degree of *LREE* enrichment over *HREE* is expressed in terms of the La_N/Yb_N value (Table 3), or the La_N/Sm_N value where Yb is below the detection limit. In addition, the chondrite-normalized *REE* patterns of many calc-silicate minerals are characterized by pronounced Eu anomalies: both positive (*e.g.*, clinozoisite, epidote, and vesuvianite) and negative (*e.g.*, monticellite and merwinite; Fig. 1).

DISCUSSION

The *REE* characteristics in calc-silicate minerals must be a reflection of partitioning among minerals and fluids if equilibrium was attained. Ideally, the partitioning of *REE* between coexisting minerals should be analyzed in order to evaluate the intrinsic and external controls on the *REE* characteristics in calc-silicate minerals. Recently, several micro-analytical methods (*e.g.*, secondary-ion mass spectrometry and laser ablation ICP–MS) have been applied successfully to determine *in situ* low levels of *REE* in some minerals, but these methods are not suitable for most calc-silicate minerals of our suite because of a lack of well-characterized mineral standards. In fact, this study represents a first attempt of providing high-quality data for low levels of *REE* in most of the metamorphic and hydrothermal calc-silicate minerals (*cf.* Grauch 1989). Our samples of calc-silicate minerals are exhibit-quality specimens, mainly from monomineralic veins and vesicles; they thus provide high-precision data on the levels of *REE*, as obtained by ICP–MS on bulk samples, without serious problems of contamination, which is inevitable with bulk analyses of minerals in fine- to medium-grained rocks. Moreover, the monomineralic nature of most of our samples allows a rather straightforward examination of factors controlling the distribution of *REE* in calc-silicate minerals based on partitioning with coexisting hydrothermal fluids only.

Aspects of *REE* crystal-chemistry have been reviewed recently by Fleet & Pan (1995a). The trivalent *REE* are almost exclusively restricted to the Ca site(s) in calc-silicate minerals (Dollase 1971, Morris 1975, Aslani-Samin *et al.* 1987, Fleet & Pan 1995a, b). The substitution of trivalent *REE* for divalent Ca requires a charge-distribution compensating mechanism to maintain electrostatic neutrality. Studies of *REE* in rare-earth minerals (*e.g.*, allanite) and *REE*-rich minerals (*e.g.*, apatite and titanite) have revealed a wide variety of possible coupled substitutions for the accommodation of trivalent rare-earth elements in the divalent Ca site(s) (Table 5).

The accommodation of the trivalent *REE* cations in a site dominated by Ca^{2+} is expected to have a significant bearing on the fractionation of *REE* by minerals. In this respect, a comparison of Ca^{2+} site stereochemistry, mechanisms of substitution and uptake of Eu^{2+} provides insight. For example, in the presence of a reduced basaltic melt, Eu^{2+} exhibits compatible behavior in plagioclase (*e.g.*, McKay 1989). This is commonly attributed to the camouflaging of Eu^{2+} by Sr^{2+}. However, the appreciably weaker partitioning of the trivalent *REE* (which are incompatible elements in plagioclase) cannot be attributed to inferior compatibility with respect to ionic size alone. The large-cation positions in plagioclase are all bonded to bridging oxygen atoms, and the bonding of a single oxygen atom to three highly charged cations (Si^{4+}, Al^{3+}, REE^{3+}) is energetically unfavorable. Thus, minerals with framework structures and large cation

TABLE 5. SCHEMES OF SUBSTITUTION BETWEEN REE AND Ca IN REE-RICH MINERALS

Substitution	Example
$2Ca^{2+} = Na^{1+} + REE^{3+}$	apatite, burbankite, fluorite
$3Ca^{2+} = 2REE^{3+} + \square$	allanite, apatite
$Ca^{2+} + (OH,F)^{-} = REE^{3+} + O^{2-}$	allanite, apatite
$Ca^{2+} + P^{5+} = REE^{3+} + Si^{4+}$	apatite, xenotime, zircon
$Ca^{2+} + H_2O = REE^{3+} + (OH)^{-}$	ancylite
$Ca^{2+} + (Al,Fe)^{3+} = REE^{3+} + (Mg,Fe)^{2+}$	allanite, dissakisite
$Ca^{2+} + B^{3+} = REE^{3+} + Be^{2+}$	gadolinite
$Ca^{2+} + Si^{4+} = REE^{3+} + B^{3+}$	melanocerite
$Ca^{2+} + Ti^{4+} = REE^{3+} + Fe^{3+}$	titanite
$2Ca^{2+} + Ti^{4+} = 2REE^{3+} + Fe^{2+}$	titanite
$Ca^{2+} + (Th,U)^{4+} = 2REE^{3+}$	monazite, uraninite
$Ca^{2+} + (Nb,Ta)^{5+} = REE^{3+} + Ti^{4+}$	euxenite, polycrase

After Cesbron (1989), Miyawaki & Nakai (1993), and Fleet & Pan (1994).

sites that normally accommodate univalent and divalent cations are not likely to readily host trivalent *REE*.

In contrast, nonbridging oxygen atoms offer opportunities for oxygen ligands to equalize their bond valence through coupled substitutions. We therefore anticipate that orthosilicates (and orthophosphates) will more readily accommodate REE^{3+} by substitutions for Ca^{2+}.

The substitution of trivalent *REE* for divalent Ca undoubtedly results in some distortion of the Ca site(s) and, possibly, changes in the crystal's symmetry also. The latter is exemplified by the apatite–britholite series. The substitution of major amounts of *REE* results in a reduction from hexagonal (uniaxial) symmetry in apatite to monoclinic (biaxial) in britholite, because of the change of the geometry of coordination polyhedra (Hughes *et al.* 1992). However, the substitution of trace amounts of *REE*, as in the metamorphic and hydrothermal calc-silicate minerals of this study, is unlikely to cause a significant change in the geometry of coordination polyhedra. Therefore, the stereochemical environments of Ca sites in end-member calc-silicate minerals may provide useful information on the site preference of *REE* in these minerals. In this study, we divide the calc-silicate minerals into two groups on the basis of the number of nonequivalent Ca sites, one group with a single Ca site, and the other with multiple Ca sites.

TABLE 6. STEREOCHEMICAL ENVIRONMENT OF Ca IN SINGLE-Ca-SITE CALC-SILICATE MINERALS

Mineral	Anion	CN	<Ca-A> (Å)
Akermanite	O	8	2.577
Andradite	O	8	2.433
Apophyllite	O,OH,F	7	2.422
Datolite	O,OH	8	2.486
Diopside	O	8	2.498
Gehlenite	O	8	2.563
Grossular	O	8	2.405
Ilvaite	O,OH	7	2.407
Margarite	O,OH	6	2.455
Monticellite	O	6	2.364
Prehnite	O,OH	7	2.460
Stilbite	H_2O	8	2.471
Scapolite	O	9	2.600
Titanite	O,OH,F	7	2.458
Tremolite	O	8	2.518

Data are mainly from Smyth & Bish (1988) and references therein.

Calc-silicate minerals with a single Ca position

The stereochemical environments of the Ca site in the calc-silicate minerals considered here as having a single Ca position are summarized in Table 6. The Ca site in these calc-silicate minerals varies in coordination number (CN) from 6 to 9 and includes various anions, such as O, OH, and F (Table 6). It is difficult, therefore, to precisely quantify the relative size of the Ca site among these minerals. In this study, the mean bond-distance <Ca–*A*> is taken as a first approximation for comparison with the degree of fractionation between *LREE* and *HREE* (La_N/Yb_N). Figure 2 shows that minerals with mean <Ca–*A*> distances shorter than ~2.4 Å are *HREE*-selective (*e.g.*, grossular and monticellite), whereas those with <Ca–*A*> distances longer than ~2.4 Å are *LREE*-selective (*e.g.*, åkermanite, gehlenite and scapolite). However, the La_N/Yb_N ratio correlates only weakly with <Ca–*A*> distance; this clearly points to the influence of external factors in controlling or modifying the *REE* patterns of some of these minerals. Moreover, several minerals with <Ca–*A*> distances between 2.4 to 2.5 Å are known to have weak selectivities among *REE*. Titanite, with a <Ca–*A*> distance of 2.458 Å, for example, has only a weak preference for *LREE*, and its *REE* characteristics in igneous rocks are dominated by provenance (Fleischer 1978, Pan *et al.* 1993). The titanite selected for this study, from a markedly *LREE*-enriched granitic pegmatite, is enriched in *LREE* relative to *HREE* (La_N/Yb_N = 4.1; Fleischer 1978, Russell *et al.* 1994).

Garnet is well known for its marked enrichment in *HREE* relative to *LREE*, because of the similarity in size of the dodecahedrally coordinated site with ideal *HREE*–oxygen distances (*e.g.*, Schwandt *et al.* 1993). The grossular of Asbestos, Quebec is characteristically enriched in *HREE* over *LREE* (La_N/Yb_N = 0.02; Fig. 1c). However, the andradite of San Benito, California, is enriched in *LREE* relative to *HREE* (La_N/Yb_N = 1.4; Fig. 1f). We suggest that the *LREE*-enriched pattern of our sample of andradite is indicative of an external control (*i.e.*, composition of fluid), because its coexisting diopside is slightly enriched in *LREE* (Fig. 1f), whereas in general clinopyroxene is known to preferentially incorporate the middle *REE* in magmatic systems (*e.g.*, McKay 1989).

Calc-silicate minerals with multiple Ca positions

Many calc-silicate minerals have structures wih multiple nonequivalent Ca positions. Therefore, the degree of order is important in understanding the behavior of *REE* in these minerals. To date, the degree of order has not been extensively studied, because of the inability of conventional diffraction methods to distinguish between individual elements on multiply-occupied sites. However, it should be possible to predict the site preference of trace elements, especially of a chemically similar group of elements

such as the *REE*, for Ca sites on the basis of the stereochemical environments of the host minerals. Morris (1975) suggested that Gd^{3+} is incorporated in a site where the crystal electric field is disordered. Smyth & Bish (1988) noted that a variation in electrostatic energy with mean cation–anion distances may be a potentially useful indicator of substitution sites of minor elements. Smyth & Bish (1988) also suggested that sites tend to favor substitutions that minimize distortions of the sites. Fleet & Pan (1994, 1995b) pointed out that in apatite, occupancy of the anion position by F, Cl and OH must exert significant control on the site preference of *REE* over two structurally nonequivalent Ca sites.

Similarly, bond-valence requirements have been suggested as an important control on *REE* site preference in minerals with multiple Ca positions, such as apatite and cuspidine (Hughes *et al.* 1991, Fleet & Pan 1994, 1995b). Therefore, calculated bond-valence should be a first-approximation technique to deduce site preference of *REE* in end-member calc-silicate structures. Bond-valence calculations are based on the bond-distance – bond-strength correlation (*e.g.*, Brown 1981), and therefore also embody a component due to variation in size of structural positions. This coupling of the effects of bond valence and size gives rise to ambiguity in interpretation that is particularly troublesome where bond valence is calculated for multiply-occupied sites, for which the experimental bond-distance is biased toward that of the substituent with the stronger X-ray scattering contribution.

There is commonly also ambiguity in defining the effective bonding sphere of Ca in calc-silicate minerals. It is clearly not practical in a multisite structure to do this by including only distances up to a bond-strength sum (s) of 2.0 valence unit (*vu*). The structure of Fe-rich epidote (Gabe *et al.* 1973) is a good example. The <Ca1–O> distance of the *A*1 site is 2.586 Å (s = 2.06 *vu*) for CN = 9 and Ca–O distance up to 3.00 Å, but is 2.468 Å (s = 1.89 *vu*) for CN = 7 and Ca–O distance up to 2.86 Å; and the <Ca2–O> distance of the *A*2 site is 2.674 Å (s = 1.84 *vu*) for CN = 10 and Ca–O distance up to 3.02 Å, but is 2.588 Å (s = 1.67 *vu*) for CN = 8 and Ca–O distance up to 2.78 Å. Therefore, we would not expect the present analysis that is based on the estimated size of Ca position and bond strength to have more than qualitative application. This ambiguity is particularly troublesome for framework structures, where a case can be made for an extended bonding sphere for the cations occupying the large cavity. For example, in the structure of anorthite of Wainwright & Starkey (1971), bond-strength sums of the four Ca positions range from 1.60 to 1.78 *vu* for Ca–O distances less than 3.0 Å. Moreover, with a bonding sphere extended to 3.5 Å, all four Ca positions remain significantly underbonded.

A comparison of structural environments (coordination number, anions, average bond-distance, bond-strength sum, electrostatic energy, and distortion index) of Ca sites in calc-silicate minerals with multiple Ca positions is given in Table 7. Fleet & Pan

TABLE 7. STEREOCHEMICAL ENVIRONMENTS OF Ca IN CALC- SILICATE MINERALS WITH MULTIPLE Ca SITES

Mineral	Site	CN	A	<Ca-A> (Å)	s (v.u.)	EE (eV)	Δ (10^{-3})
Anorthite	A(000)	6	O	2.454	1.60	-41.6	11.7
	A(z00)	8	O	2.597	1.78	-41.5	14.9
	A(0i0)	7	O	2.503	1.70	-41.3	20.5
	A(zi0)	7	O	2.538	1.63	-42.3	30.9
Axinite	Ca1	6	O	2.416	1.72		8.45
	Ca2	6	O,OH	2.393	1.84		12.7
Bustamite	M1	6	O	2.348	2.01	-44.9	6.94
	M2	6	O	2.371	1.90	-43.1	6.74
	M4	8	O	2.490	1.98	-43.5	12.6
Clinozoisite	A1	9	O	2.575	2.03	-45.7	27.3
	A2	10	O,OH	2.672	1.70	-41.6	55.7
Epidote	A1	9	O	2.586	2.06	-46.5	26.4
	A2	10	O,OH	2.674	1.84	-41.7	74.9
Larnite	Ca1	7	O	2.51	1.74		37.9
	Ca2	8	O	2.49	1.94		12.5
Merwinite	Ca1	8	O	2.556	1.84		42.9
	Ca2	9	O	2.588	1.93		36.2
	Ca3	8	O	2.582	1.67		20.6
Pectolite	M1	6	O,OH	2.368	1.88		1.51
	M2	6	O,OH	2.360	1.92		2.17
Spurrite	Ca1	8	O	2.529	1.86		22.5
	Ca2	8	O	2.527	1.85		19.4
	Ca3	8	O	2.484	1.99		11.2
	Ca4	7	O	2.429	2.02		19.4
	Ca5	7	O	2.435	1.92		6.3
Tilleyite	Ca1	6	O	2.404	1.74		1.3
	Ca2	7	O	2.441	1.92		13.1
	Ca3	7	O	2.487	1.71		11.2
	Ca4	6	O	2.371	1.91		4.6
	Ca5	6	O	2.408	1.77		9.5
Vesuvianite	X1	8	O	2.442	2.18	-32.7	8.19
	X2	7	O	2.472	2.12	-37.3	31.4
	X3	8	O,OH	2.504	1.88	-50.5	4.92
	C	8	O	2.464	2.20	-4.6	20.7
Wollastonite	M1	6	O	2.373	1.91	-33.2	10.5
	M2	6	O	2.381	1.84	-38.6	4.32
	M3	7	O	2.414	2.03	-82.7	11.8

Bond valence (s; v.u., valence unit) is calculated using the formula: $s = (R/R_o)^{-N}$, where R is bond length, R_o = 1.909 Å and N = 5.4 for bonds to oxygen (Brown 1981). The distortion parameter (Δ) is calculated using the formula:

$$\Delta = 1/N \cdot \sum_{i=1}^{N} (R_i - R_o)^2,$$

where R_i and R_o are the individual and average radii for a coordination polyhedron, respectively, and N is the coordination number (Fleet 1976). The electrostatic energy (EE) was taken from Smyth & Bish (1988).

(1994) pointed out that the Ca2 position in end-member fluorapatite is underbonded. Therefore, minor amounts of trivalent *REE* should favor Ca2 over Ca1, to increase the bond valence of Ca2. The relatively small Ca2 site of bustamite is underbonded (it also has the smallest distortion index but also the smallest electrostatic energy per charge; Table 7), consistent with an *HREE*-enriched pattern (Fig. 1c). Similarly, tilleyite has five distinct Ca sites, and three of them are significantly underbonded (Table 7). The observed convex-downward *REE* pattern of tilleyite (Fig. 1d) is consistent with preferential incorporation of *LREE* and *HREE* in these three different sites. The *X*3 site in vesuvianite is underbonded and has the highest electrostatic energy per charge (potential) and the lowest distortion index among the four Ca sites in this mineral (Table 7). Therefore, *REE* should be incorporated preferentially in the *X*3 site. Fitzgerald *et al.* (1987) have shown that *REE* are indeed incorporated preferentially in the *X*3 site in *REE*-rich vesuvianite. Also, the steep chondrite-normalized *REE* pattern is consistent with the long <Ca3–*A*> distance.

The difference in stereochemical environments of the coexisting Ca sites in some calc-silicate minerals (*e.g.*, anorthite) is very small. Therefore, complete disorder is predicted for *REE* among the Ca sites in such minerals. Morris (1975) concluded that Eu^{2+} and Gd^{3+} do occupy the Ca sites in anorthite, but was unable to differentiate between the different Ca sites. The optical spectra of Eu^{3+} in synthetic anorthite (D'Arco & Piriou 1989) revealed a large population of local sites for the *REE* cations. D'Arco & Piriou (1989) suggested that Eu^{3+} either is trapped in defects or substitutes for Ca^{2+} in distorted sites.

A control of *REE* characteristics in some calc-silicate minerals, such as larnite and pectolite, by size of Ca site is evident irrespective of a preferential incorporation among their nonequivalent Ca sites, because all Ca sites in these minerals have similar mean bond-distances. For example, the enrichment of *LREE* over *HREE* in larnite (Table 2) is consistent with the long <Ca–*A*> distances (Table 7). The chondrite-normalized pattern of our specimen of pectolite has a negative slope in the *LREE* portion (Fig. 1b), although *HREE* are below detection limits (perhaps reflecting extremely low levels of *HREE* in the fluid). The negative slope is consistent with the short <Ca–*A*> distance of both Ca sites in pectolite (Table 7). Also, Y- and *HREE*-enriched members of the pectolite–serandite series have been reported by Semenov *et al.* (1976).

Epidote-group minerals are characterized by two distinct Ca sites (*A*1 and *A*2). Rare-earth elements in allanite, dissakisite and dollaseite order at the larger *A*2 site (Dollase 1971, Peacor & Dunn 1988, Rouse & Peacor 1993). This finding is consistent with predictions based on structural environments of the two Ca sites in clinozoisite and epidote (Smyth & Bish 1988; Table 7) and has been used to explain the marked enrichment of *LREE* over *HREE* commonly observed in epidote-group minerals (Grauch 1989). Our epidote from Wollaston Township, Ontario, is characteristically enriched in *LREE* over *HREE* (Fig. 1f). However, the epidote from Munro Township, Ontario and the clinozoisite of the Hollinger mine, Timmins, Ontario show marked enrichment of *HREE* over *LREE* (Fig. 1f). At least the clinozoisite of the Hollinger mine illustrates the control of *REE* characteristics in minerals by external factors (see below).

Catapleiite

Sodium (and Ca) in catapleiite occupy large, eight-fold-coordinated sites (<Na–*A*> distances of 2.550–2.564 Å; Ilyushin *et al.* 1981). Therefore, a *LREE*-enriched chondrite-normalized pattern is expected if *REE* are restricted to these eight-fold-coordinated sites. However, the chondrite-normalized *REE* pattern of catapleiite is characterized by a convex-downward shape (Fig. 1d). This may be explained by an accommodation of *HREE* into the Zr sites (<Zr–O> distance is 2.072 Å, as in zircon: Ball 1982).

Defects and interstitial sites

Point defects and interstitial sites have been postulated to explain the distribution of trace elements in several silicate minerals, especially at very low concentrations (*e.g.*, D'Arco & Piriou 1989). However, the intrinsically controlled *REE* characteristics of the metamorphic and hydrothermal calc-silicate minerals discussed above are best explained by accommodation in the Ca site(s).

Crystal-chemical versus external controls on the REE characteristics in calc-silicate minerals

We have shown above that the *REE* characteristics of many of the calc-silicate minerals studied here (*e.g.*, åkermanite, axinite and monticellite) are consistent with a crystal-chemical control based on substitution for Ca (Fig. 2, Table 3). However, the *REE* characteristics of some calc-silicate minerals, such as clinozoisite and epidote, are opposite of those predicted by crystal chemistry; therefore, external factors must have dominated in these samples. To illustrate the external controls on the *REE* characteristics in calc-silicate minerals, coexisting calcite and associated lithologies of the clinozoisite sample from the Hollinger mine, Timmins, Ontario, have also been analyzed for *REE* by ICP–MS (Table 8).

The clinozoisite of the Hollinger mine occurs in a vein (about 40 cm wide) cross-cutting an albitized host-rock (albite, chlorite, actinolite, quartz, epidote, and titanite). The vein consists of two distinct zones: a dark-colored, fine-grained, marginal zone with

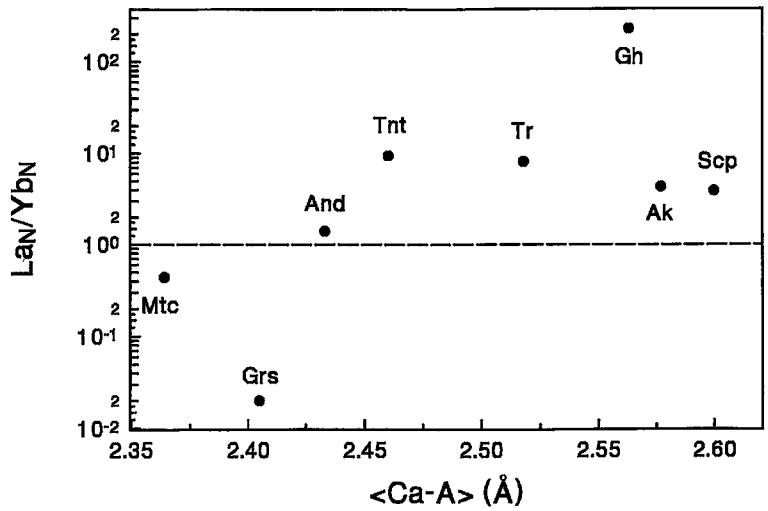

FIG. 2. Plot of La_N/Yb_N value *versus* <Ca–*A*> bond distance for calc-silicate minerals with single Ca site (see Table 3 for labels). Note that dominance by crystal-chemical factors would result in a strong positive correlation between La_N/Yb_N and <Ca–*A*>.

TABLE 8. LEVELS OF RARE-EARTH ELEMENTS IN CLINOZOISITE, CALCITE, CHLORITE-RICH MARGIN, AND ALBITIZED HOST-ROCK FROM THE HOLLINGER MINE

	clinozoisite	calcite	Chl-rich margin	albitized host-rock
La (ppm)	0.28	0	0.44	3.38
Ce	0.76	0.04	1.37	9.5
Pr	0.12	0.01	0.21	1.41
Nd	0.52	0	1.18	7.03
Sm	0.23	0.05	0.38	2.41
Eu	0.75	0.02	0.11	0.62
Gd	0.51	0.04	0.49	3.31
Tb	0.12	0.01	0.08	0.52
Dy	1.17	0.08	0.62	3.5
Ho	0.33	0.02	0.12	0.73
Er	1.45	0.14	0.38	2.22
Tm	0.25	0.03	0.06	0.3
Yb	2.02	0.53	0.34	1.76
Lu	0.34	0.13	0.06	0.25
La_N/Yb_N	0.09		0.87	1.30
Eu_N/Eu_N^*	6.69	1.37	0.78	0.67

ppm, parts per million; La_N/Yb_N, chondrite-normalized La/Yb ratio; $Eu_N^* = (Sm_N \times Gd_N)^{0.5}$.

predominant chlorite and quartz (and minor amounts of albite and clinozoisite), and a light-colored, coarse-grained, bimineralic (clinozoisite and calcite) central zone. Keys (1940) showed that the clinozoisite-bearing veins occur as part of an early stage of hydrothermal alteration in the Hollinger mine (see also Wood *et al.* 1986). The chondrite-normalized *REE* pattern of the chlorite-rich margin is slightly *HREE*-enriched (La_N/Yb_N = 0.87), whereas that of the albitized host-rock is only slightly *LREE*-enriched (La_N/Yb_N = 1.3; Fig. 3). Calcite, similar to the coexisting clinozoisite, is characterized by an enrichment in *HREE* relative to *LREE* (Ce_N/Yb_N = 0.02; Fig. 3). This confirms that the fluid responsible for the crystallization of calcite and clinozoisite was *HREE*-enriched. The *REE* present in the chlorite-rich margin may reflect the *REE* characteristics of the initial fluid, which may have been derived from or equilibrated with the albitized host-rock. Experimental and theoretical studies (*e.g.*, Cantrell & Byrne 1987, Wood 1990) have demonstrated that *HREE* complexes (carbonate, fluoride, *etc.*) are generally relatively more stable than *LREE* ones. As crystallization proceeded from the chlorite-rich margin to the clinozoisite–calcite central zone, the fluid became progressively more enriched in *HREE*, resulting in the formation of *HREE*-enriched clinozoisite and calcite.

The presence of Ce and Eu anomalies in chondrite-normalized whole-rock *REE* patterns has long been used as indicators for oxidation-reduction conditions during metamorphism and hydrothermal alterations (Grauch 1989, Lottermoser 1992; Pan *et al.* 1994). Similarly, the presence of a Eu anomaly in minerals

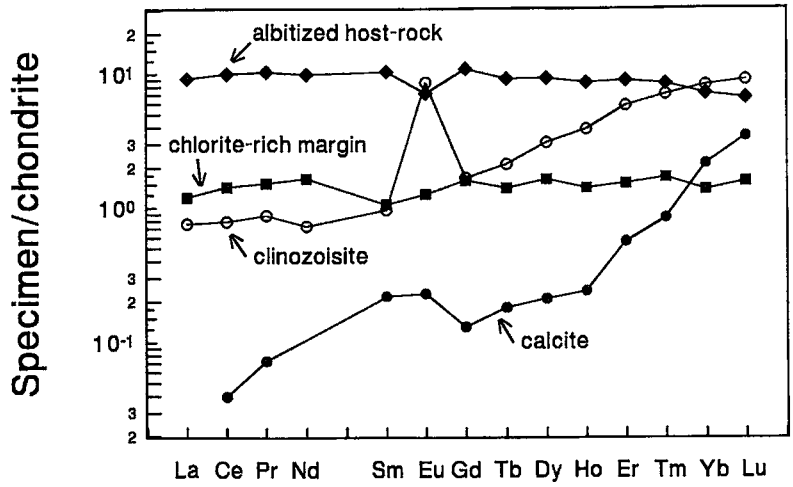

FIG. 3. Chondrite-normalized *REE* patterns of clinozoisite, calcite, chlorite-rich margin, and albitized host-rock from the Hollinger mine, Timmins, Ontario.

such as anorthite and apatite has been demonstrated experimentally by Roeder *et al.* (1987) and Aslani-Samin *et al.* (1987) to correlate directly with redox conditions. Europium anomalies are pronounced in many metamorphic and hydrothermal calc-silicate minerals in our suite (Fig. 1) and, therefore, may be used as a potential indicator of redox conditions. For example, the presence of a pronounced, positive Eu anomaly in the clinozoisite of the Hollinger mine indicates that the hydrothermal fluid responsible for its formation was reducing. Wood *et al.* (1986) suggested that the early stage of alteration in the Hollinger mine was indeed highly reducing, approaching the pyrite–pyrrhotite buffer. The coexisting calcite also shows a small, positive Eu anomaly (Fig. 3, Table 8). Previous studies have documented that hydrothermal veins (*i.e.*, bulk-rock data) in Archean gold camps of Timmins, Ontario are characterized by pronounced, positive Eu anomalies (*e.g.*, Dome mine; Kerrich & Fryer 1979), indicating highly reducing conditions, which are ideal for the transport of gold as bisulfide complexes (*cf.* Seward 1984).

Therefore, the occurrence of Eu anomaly in clinozoisite and calcite of the Hollinger mine clearly reflects the presence of Eu^{2+} in a reducing hydrothermal fluid. Yet, the difference in the magnitude of Eu anomaly (*i.e.*, partitioning of Eu^{2+}) between these two coexisting minerals is consistent with their crystal chemistry. The *A*2 site in clinozoisite is closer in effective ionic radius to Eu^{2+} than the Ca site in calcite (Shannon 1976). Therefore, clinozoisite preferentially incorporates Eu^{2+} into its structure relative to coexisting calcite, resulting in a more prominent positive Eu anomaly in the former (Table 8, Fig. 3).

Many previous studies have invoked two distinctly different types of control to explain fractionation between *LREE* and *HREE* in hydrothermal alteration, either 1) internally by crystal chemistry or 2) externally by geochemical factors, such as temperature, pressure, and preferential complexation of *HREE* with F, particularly at high temperatures (Wood 1990, Fleet & Pan 1995b). We emphasize that these two types of controls are in fact not independent and must act together determining the overall *REE* characteristics of minerals (*e.g.*, pectolite of this study) during growth, although dominance of one over the other is clearly present in individual cases.

CONCLUSIONS

1) Twenty nine calc-silicate minerals and catapleiite have been analyzed by ICP–MS; for the rare-earth elements. *REE* patterns for many metamorphic and hydrothermal calc-silicate minerals with low abundances of *REE* are reported for the first time.

2) The *REE* characteristics of many calc-silicate minerals are consistent with a crystal-chemical control based on substitution for Ca. However, the *REE* characteristics of some calc-silicate minerals are clearly dominated by external factors, and can be used to estimate the physicochemical conditions of coexisting hydrothermal fluids.

3) Bond-valence calculation is a powerful first-approximation technique for predicting the site preference of *REE* in calc-silicate minerals with multiple Ca sites.

ACKNOWLEDGEMENTS

We thank two unnamed referees for incisive criticism and helpful suggestions, and R.F. Martin and M.R. St-Onge for editorial assistance. We also thank L.D. Coleman for permission to sample the mineral collection of the University of Saskatchewan, and T. Bonli and J. Jain for analytical assistance. Financial support to this study was provided by a President's NSERC Fund from the University of Saskatchewan.

REFERENCES

ASLANI-SAMIN, S., BINCZYDKA, H. & HAFNER, S.S. (1987): Crystal chemistry of europium in feldspars. *Acta Crystallogr.* **A43** (*Suppl.*), C155 (abstr.).

AYERS, J.C. & WATSON, E.B. (1993): Apatite/fluid partitioning of rare-earth elements and strontium: experimental results at 1.0 GPa and 1000°C and application to models of fluid–rock interaction. *Chem. Geol.* **110**, 299-314.

BALL, D. (1982): The paramagnetic resonance of Nd^{3+} and Yb^{3+} in zircon structure silicates. *Phys. Status Solidi (b)* **111**, 311-320.

BROWN, I.D. (1981): The bond-valence method: an empirical approach to chemical structure and bonding. *In* Structure and Bonding in Crystals **2** (M. O'Keeffe & A. Navrotsky, eds.). Academic Press, New York, N.Y. (1-30).

CANTRELL, K.J. & BYRNE, R.H. (1987): Rare earth element complexation by carbonate and oxalate ions. *Geochim. Cosmochim. Acta* **51**, 597-605.

CESBRON, F. (1989): Mineralogy of the rare-earth elements. *In* Lanthanides, Tantalum and Niobium (P. Möller, P. Černý & F. Saupé, eds.). Springer-Verlag, Berlin, Germany (3-26).

D'ARCO, P. & PIRIOU, B. (1989): Fluorescence spectra of Eu^{3+} in synthetic polycrystalline anorthite: distribution of Eu^{3+} in the structure. *Am. Mineral.* **74**, 191-199.

DOLLASE, W.A. (1971): Refinement of the crystal structures of epidote, allanite and hancockite. *Am. Mineral.* **56**, 447-464.

FITZGERALD, S., LEAVENS, P.B., RHEINGOLD, A.L. & NELEN, J.A. (1987): Crystal structure of a *REE*-bearing vesuvianite from San Benito County, California. *Am. Mineral.* **72**, 625-628.

FLEET, M.E. (1976): Distortion parameters for coordination polyhedra. *Mineral. Mag.* **40**, 531-533.

_____ & PAN, YUANMING (1994): Site preference of Nd in fluorapatite [$Ca_{10}(PO_4)_6F_2$]. *J. Solid State Chem.* **112**, 78-81.

_____ & _____ (1995a): Crystal chemistry of rare earth elements in fluorapatite and some calc-silicates. *Eur. J. Mineral.* **7**, 591-605.

_____ & _____ (1995b): Site preference of rare earth elements in fluorapatite. *Am. Mineral.* **80**, 329-335.

FLEISCHER, M. (1978): Relations of the relative concentrations of lanthanides in titanite to type of host rocks. *Am. Mineral.* **63**, 869-873.

GABE, E.J., PORTHEINE, J.C. & WHITLOW, S.H. (1973): A reinvestigation of the epidote structure: confirmation of the iron location. *Am. Mineral.* **58**, 218-223.

GOVINDARAJU, K. (1989): 1989 compilation of working values and sample description for 272 geostandards. *Geostandards Newslett.* **13** (*spec. issue*), 1-113.

GRAUCH, R.I. (1989): Rare earth elements in metamorphic rocks. *In* Geochemistry and Mineralogy of Rare Earth Elements (B.R. Lipin & G.A. McKay, eds.). *Rev. Mineral.* **21**, 147-167.

HUGHES, J.M., CAMERON, M. & MARIANO, A.N. (1991): Rare-earth-element ordering and structural variations in natural rare-earth-bearing apatites. *Am. Mineral.* **76**, 1165-1173.

_____, MARIANO, A.N. & DREXLER, J.W. (1992): Crystal structures of synthetic Na–*REE*–Si oxyapatites, synthetic monoclinic britholite. *Neues Jahrb. Mineral., Monatsh.*, 311-319.

ILYUSHIN, G.D., VORONKOV, A.A., ILYUKHIN, V.V., VEVSKII, N.N. & BELOV, N.V. (1981): Crystal structure of natural monoclinic catapleiite $Na_2ZrSi_3O_9{\cdot}2H_2O$. *Sov. Phys. Dokl.* **26**, 808-810.

JENNER, G.A., LONGERICH, H.P., JACKSON, S.E. & FRYER, B.J. (1990): ICP–MS – a powerful tool for high-precision trace-element analysis in Earth Sciences: evidence for analysis of selected U.S.G.S. reference samples. *Chem. Geol.* **83**, 133-148.

KERRICH, R. & FRYER, B.J. (1979): Archean precious-metal hydrothermal systems, Dome mine, Abitibi greenstone belt. II. *REE* and oxygen isotope relations. *Can. J. Earth Sci.* **16**, 440-458.

KEYS, M.R. (1940): Paragenesis in the Hollinger veins. *Econ. Geol.* **35**, 611-628.

KRETZ, R. (1983): Symbols for rock-forming minerals. *Am. Mineral.* **68**, 277-279.

LOTTERMOSER, B.G. (1992): Rare earth elements and hydrothermal ore formation processes. *Ore Geol. Rev.* **7**, 25-41.

MCKAY, G.A. (1989): Partitioning of rare earth elements between major silicate minerals and basaltic melts. *In* Geochemistry and Mineralogy of Rare Earth Elements (B.R. Lipin & G.A. McKay, eds.). *Rev. Mineral.* **21**, 45-77.

MIYAWAKI, T. & NAKAI, I. (1993): Crystal-chemical aspects of rare-earth minerals. *In* Rare Earth Minerals: Chemistry, Origin and Ore Deposits. Mineral. Soc. Great Britain and Ireland, National History Mus. London, Abstr., 86-88.

MÖLLER, P. & MORTEANI, G. (1983): On the geochemical fractionation of rare earth elements during the formation of Ca-minerals and its application to problems of the genesis of ore deposits. *In* The Significance of Trace Elements in Solving Petrogenetic Problems and Controversies (S.S. Augustithis, ed.). Theophrastus Publ., Athens, Greece (747-791).

MORRIS, R.V. (1975): Electron paramagnetic resonance study of the site preferences of Gd^{3+} and Eu^{2+} in polycrystalline silicate and aluminate minerals. *Geochim. Cosmochim. Acta* **39**, 621-634.

MORSS, L.R. (1976): Thermochemical properties of yttrium, lanthanum, and the lanthanide elements and ions. *Chem. Rev.* **76**, 827-841.

PAN, YUANMING, FLEET, M.E. & MACRAE, N.D. (1993): Late alteration in titanite ($CaTiSiO_5$): redistribution and remobilization of rare earth elements and implications for U/Pb and Th/Pb geochronology and nuclear waste disposal. *Geochim. Cosmochim. Acta* **57**, 355-367.

_____, _____ & BARNETT, R.L. (1994): Rare earth mineralogy and geochemistry of the Mattagami Lake volcanogenic massive sulfide deposit, Quebec. *Can. Mineral.* **32**, 133-147.

PEACOR, D.R. & DUNN, P.J. (1988): Dollaseite-(Ce) (magnesium orthite redefined): structure refinement and implications for $F^+ + M^{2+}$ substitution in epidote-group minerals. *Am. Mineral.* **73**, 838-842.

ROEDER, P.L., MACARTHUR, D., MA, XIN-PEI, PALMER, G.R. & MARIANO, A.N. (1987): Cathodoluminescence and microprobe study of rare-earth elements in apatite. *Am. Mineral.* **72**, 801-811.

ROUSE, R.C. & PEACOR, D.R. (1993): The crystal structure of dissakisite-(Ce), the Mg analogue of allanite-(Ce). *Can. Mineral.* **31**, 153-157.

RUSSELL, J.K., GROAT, L.A. & HALLERAN, A.A.D. (1994): *LREE*-rich niobian titanite from Mount Bisson, British Columbia: chemistry and exchange mechanisms. *Can. Mineral.* **32**, 575-587.

SCHWANDT, C.S., PAPIKE, J.J., SHEARER, C.K. & BREARLEY, A.J. (1993): A SIMS investigation of *REE* geochemistry of garnet in garnetite associated with the Broken Hill Pb–Zn–Ag orebodies, Australia. *Can. Mineral.* **31**, 371-379.

SEMENOV, E.I., MAKSIMYUK, I.E. & ARKANGELSKAYA, V.N. (1976): On the minerals of the pectolite–serandite group. *Zap. Vses. Mineral. Obshchest.* **104**, 154-163. (in Russ.).

SEWARD, T.M. (1984): The transport and deposition of gold in hydrothermal systems. *In* Gold'82: the Geology, Geochemistry and Genesis of Gold Deposits (R.P. Foster, ed.). Balkema, Rotterdam, The Netherlands (165-181).

SHANNON, R.D. (1976): Revised effective ionic radii and systematic studies of interatomic distances in halides and chalcogenides. *Acta Crystallogr.* **A32**, 751-767.

SMYTH, J.R. & BISH, D.L. (1988): *Crystal Structures and Cation Sites of the Rock-Forming Minerals.* Allen & Unwin, Boston, Massachusetts.

TAYLOR, S.R. & MCLENNAN, S.M. (1985): *The Continental Crust: its Composition and Evolution.* Blackwell Scientific Publ., Oxford, U.K.

WAINWRIGHT, J.E. & STARKEY, J. (1971): A refinement of the structure of anorthite. *Z. Kristallogr.* **133**, 75-84.

WOOD, P.C., BURROWS, D.R., THOMAS, A.V. & SPOONER, E.T.C. (1986): The Hollinger–McIntyre Au – quartz vein system, Timmins, Ontario, Canada; geologic characteristics, fluid properties and light stable isotope geochemistry. *In* Proc. Gold'86, an International Symposium on the Geology of Gold (A.J. Macdonald, ed.). Konsult International Inc., Willowdale, Ontario (56-80).

WOOD, S.A. (1990): The aqueous geochemistry of the rare-earth elements and yttrium. 2. Theorectical predictions of speciation in hydrothermal solutions to 350°C at saturation water vapor pressure. *Chem. Geol.* **88**, 99-125.

XIE, QIANLI, JAIN, J., SUN, MIN, KERRICH, R. & FAN, JIANZHONG (1994): Multi-element analysis of low abundance international reference material BIR–1: results by ICP–MS. *Geostandards Newslett.* **18**, 53-63.

Received March 22, 1995, revised manuscript accepted September 21, 1995.